Spanish Journal of Agricultural Research
20 (1), e0202, 15 pages (2022)
eISSN: 2171-9292
https://doi.org/10.5424/sjar/2022201-18499
INIA-CSIC

RESEARCH ARTICLE

OPEN ACCESS

Effect of potato contact parameters on seed metering performance using discrete element method

Linrong Shi, Xiaoping Yang, Wuyun Zhao, Bugong Sun, Guanping Wang, and Wei Sun
College of Mechanical and Electrical Engineering, Gansu Agricultural University, Lanzhou 730070, China

Abstract

Aim of study: To study the effect of potato surface with or without sandy loam soil on seed metering performance, we investigated the motion behaviour of the potato seed particles during the seed metering process using a self-designed across-bridge metering device by discrete element method (DEM).

Area of study: Tonganyi Town, Dingxi, Gansu, China

Material and methods: First, the contact characteristics of potatoes were measured using some novel devices. Second, simulations were performed under the same experimental conditions to verify the reliability of the contact parameters. Finally, the velocity and angular velocity of the seed in the seed box and the number of seeds taken by the large spoon during the taking and clearing process were analysed using ANOVA.

Main results: The coefficients of static friction (SF) and rolling friction (RF) of seed particles with soil were smaller than those without soil and had the highest values between particles and plastic, followed by between particles and steel, and between particles. Further, the rates of metering single seed particle in simulation and experiment were 98.17% and 97.57%, respectively. The rate of missing seed particles was 1.83% and 2.43%, respectively; it was found to significantly decrease as RF increased from 0.01 to 0.06 to 0.12, and the resultant angular velocity and velocity also significantly decreased as SF increased from 0.1 to 0.5 to 1.0. In addition, the number of seeds taken by the large spoon also reduced.

Research highlights: Therefore, potato seed particles surface with or without soil can significantly affect the seeding performance and highlight the need for surface treatment using mechanised metering.

Additional key words: coefficient of rolling friction; coefficient of static friction; potatoes with or without soil; simulation

Abbreviations used: DEM (discrete element method); RF (rolling friction); SF (static friction). **Nomenclature:** a (indices for particle or implement); b (indices for particle or implement); D (qualified rate of single seed, %); e (coefficient of restitution); E_a (Young's modulus for particles a); E_b (Young's modulus for particles b); E_{eq} (equivalent Young's modulus); f (shape index); F_n (normal force); F_{res} (resultant force, N); F_t (tangential force); F_n^s (normal contact force, N); F_n^d (normal damping force, N); F_t^s (tangential contact force, N); F_t^d (tangential damping force, N); g (gravitational acceleration, m s^{-2}); G_a (shear modulus for the particles a, Pa); G_b (shear modulus for the particles b, Pa); G_{eq} (equivalent shear modulus, Pa); H (drop heights of potato, m); h (rebound heights of potato, m); K_n (normal stiffness, N m^{-1}); K_t (tangential stiffness, N m^{-1}); L (maximum length of potato seeds, mm); m (mass, kg); M (moment, Nm); M_1 (rate of missing seed, %); m_1 (mass of the water and bucket, kg); m_a (mass of the particles a, kg); m_b (mass of the individual particles b, kg); m_{eq} (equivalent mass, kg); M_r (moment due to rolling friction, N m); M_{res} (resultant moment, N m); r_a (radius of particles a, m); r_b (radius of particles b, m); r_{con} (perpendicular distance of the contact point from the centre of mass, m); r_{eq} (equivalent radius, m); T (maximum height of potato seeds, mm); U_{abn} (normal component of the relative displacement); U_{abt} (tangential component of the relative displacement, m); $\ddot{U}$ (translational acceleration, m s^{-2}); v_a (Poisson's ratio for particles a); v_b (Poisson's ratio for particles b); v_n (normal velocities of potato before collision, m s^{-1}); W (maximum width of potato seeds, mm); x (coefficient of rolling friction); y (repose angle, °); $\lambda_{\dot\theta}$ (unit vector of angular velocity at the contact point); μ (friction coefficient); μ_n (normal velocities of potato after collision, m s^{-1}); μ_r (coefficient of rolling friction); $\dot\theta$ (angular velocity, rad s^{-1}), $\ddot\theta$ (rotational acceleration rad s^{-2})

Authors' contributions: Conceived, designed and performed the experiments: LRS. Designed and performed the experiments: XPY. Analysed the experiments data: WYZ. Contributed some novel ideas: BGS., GPW and WS. All authors read and approved the final manuscript.

Citation: Shi, LR; Yang, XP; Zhao, WY; Sun, BG; Wang, GP; Sun, W (2022). Effect of potato contact parameters on seed metering performance using discrete element method. Spanish Journal of Agricultural Research, Volume 20, Issue 1, e0202. https://doi.org/10.5424/sjar/2022201-18499

Received: 7 Jun 2021. **Accepted:** 20 Jan 2022.

Funding agencies/institutions	Project / Grant
Excellent PhD Thesis Cultivation Project of Gansu Agricultural University	YB2020003
National Natural Science Foundation of China	52065004

Competing interests: The authors have declared that no competing interests exist.

Correspondence Wuyun Zhao: zhaowy@gsau.edu.cn and Linrong Shi: shilr@gsau.edu.cn (shared corresponding authors)

Introduction

Potato is the largest non-cereal food crop in plant area (Zhang *et al.*, 2017) and ranks the fourth most important food crop after rice, wheat, and corn in acreage, yield, and value. With the rapid global development of the potato industry in recent years, the scale of potato crop production in China has also expanded. Although China currently accounts for the world's largest potato cultivation area and total production, the production level is still far behind that of other developed countries, such as the USA and Germany (Li, 2008). Mechanised production is a critical factor limiting the development of the potato industry in China (Lv *et al.*, 2015).

The mechanised metering process, the key to achieving mechanised production, directly affects the potato yield and quality (Du *et al.*, 2011). Potato precision metering technology can improve operational efficiency, save cost, and is irreplaceable in the seeder (Lu, 2015). The seeders can be pneumatic or mechanical, depending on the working principle (Hou *et al.*, 2018). Mechanical seeders have the advantages of low requirements of seed shape, few damages to seed, and better adaptability, but its structure is complicated and unreliable. Simple structures, low cost, and ease of maintenance make mechanical feeders the most preferred type. Mechanical feeders are classified as spoon belt (chain) type, spoon disc type, and pinch type (Wang YX *et al.*, 2016). The spoon disc type has better versatility but unstable metering uniformity and poor reliability, while the pinch type can significantly damage the potatoes. The spoon-chain device is more widely adopted due to its high reliability and versatility. However, if the potato seed in the seed box is not filled in time, problems such as missing seeds and decreasing picking rate with increasing chain speed can occur (Buitenwerf *et al.*, 2006), resulting in decreased production (up to 7%) (Liu *et al.*, 2016). Studies on improving the metering performance of the spoon-chain metering device suggest limiting the seed velocity, increasing the seed filling height, and adding vibration devices to improve the seed filling rate (Hamid *et al.*, 2010; Al-Gaadi & Marey, 2011; Niu *et al.*, 2016). However, these studies do not address the key technical questions of inadequate seed collection addressed by Yang (2014). Missing seeds can be linked to the metering form, device structural parameters, seed shape, and flow characteristics of the seed population. In 2019, our research group designed a new type of potato cross-bridge metering device, which contained large scoops that could pick more than one seed and small scoops holding a single seed. The seed transition from the large to small scoop when crossing the bridge increases the qualification metering rate of single seed.

In the past, the structure and movement of the metering device were optimised by traditional theoretical analyses and field experiments. The former faces distortion in analysing the flow characteristics of discrete materials, while the latter is both time- and labour-consuming (Yang *et al.*, 2018; Lv *et al.*, 2018). Therefore, in recent years, the discrete element method (DEM) has been used to explore the seed movement in a device and optimise the structure of devices (Li *et al.*, 2011; Owen & Cleary, 2012; Peng *et al.*, 2016). DEM is an effective tool for investigating the microscopic properties of particles when transient forces and energy dissipation cannot be investigated using conventional experimental methods (Moreno-Atanasio, 2012). It has been applied in agricultural research related to soil and seed particles, such as corn (Wang *et al.*, 2015), rice grain (Markauskas & Kaianauskas, 2011), and soybean (Yan *et al.*, 2020). DEM has been used to evaluate the metering systems (Barr *et al.*, 2019), optimise the structure and motion parameters of the metering device with upper and lower seed boxes (Niu *et al.*, 2016), explore the influences of disc rotation, flying height, and baffle ring angle of an unmanned aerial vehicle on the distribution of the centrifugal rice seeding spreader (Wu *et al.*, 2020), investigate the effects of the seed tube type and diameter, seed-dropping height and forward velocity on seed motion characteristics and seeding performance (Lei *et al.*, 2021), and simulate the effect of particle shape on motion and mixing in a rotary batch seed coaters (Pasha *et al.*, 2016). DEM has also been applied to calibrate the contact parameters of mini potatoes using experiment and simulation methods (Liu *et al.*, 2018). Gao & Xie (2019) studied the 4GS-1500 type rod chain elevator potato soil separation mechanism using DEM to optimise the design and motion parameters. However, potato seed particles contact parameters also influence the flow process, and their effect on the working performance of seed metering device has not been studied so far.

The potato seed particles surface with or without soil can alter two important contact parameters, the coefficient of rolling friction (RF) and the coefficient of static friction (SF), and further affect the metering seed performance. Therefore, this study investigates the influence of the potato contact characteristic parameters on seed metering performance of the designed across-bridge potato metering device using DEM. Firstly, the RF and SF of the seed particles with and without soil particles on their surface were measured by the proposed device; further, we investigated in detail the effect of RF and SF on the velocity and angular velocity of seed particles in the seed box, the number of potatoes picked by a large spoon, and seed clearing by a potato cross-bridge metering device.

Material and methods

Because the soil attached to the potato skin will affect the potato contact parameters, it is necessary to differentiate the motion behaviour and flow of potatoes with and without soil. In addition, the soil volume can also influence the contact parameters. To investigate the effect of RF and SF on the seed metering performance of the proposed device, we divided the potatoes into two types, (i) natural potato with soil and (ii) washed with water. The dirt in the water-washed seed particles was dried to measure the soil quantity and particle size. The average soil carrying capacity of potato was 0.01 g, and the particle size was 0.001-0.03 mm.

Potato metering device

The potato cross-bridge metering device mainly consists of the seed box, seed picking spoon assembly, spoon chain frame, seed carrying box, and seed separator (Fig. 1a). It is further divided into four functional units (Fig. 1b), the seed-collecting stage, bridging stage to clear excess potatoes, seed carrying stage, and zero-speed throwing seed stage. The working of the device is as follows: with the transmission of the drive chain, the large seed spoon picks more than one potato from the bottom to the top of the seed box (Zone I). When the seed spoon assembly passes through Sprocket I, particles slide down to the small spoon along its circular track. Subsequently, when it passes through Zone II, the extra particles slide back into the seed box, while those in the small spoon continue to move along the drive chain. When it reaches Zone IV, the seed is metered out. The seed picking spoon assembly consists of 12 small and large spoons placed along the drive chain (1828.8 mm in length). The semi-spherical small spoon has a maximum diameter of 59 mm and a depth of 22 mm, with a circular hole of 15 mm at its bottom. The semicylindrical large spoon has a diameter of 59 mm, length of 90 mm, and thickness of 22 mm. The spoons are placed such that they are vertically facing each other. The space between the seed spoon assemblies is 152.4 mm, the horizontal speed of the metering device is 0.56-1.39 m s^{-1}, and the velocity of the drive chain is 0.26-0.64 m s^{-1}. For simulation, 310 particles are generated in the seed box (Fig. 1c-d). The total simulation time is set at 20 s in steps of 1.11×10^{-4}s and the drive chain is set at 0.6 m s^{-1}. For reducing simulation time, parts of the metering device not involved in the metering process are not simulated.

The simulation detects the active level of seed particles in the seed box, number of large scoops taken, and rate of seed clearing to explain the influence of friction coefficients on seed metering performance. The three detection areas, to detect population activity, potato number, and clear potato (Fig. 1e-f), provide velocity, angular velocity, and the number crossing respectively. The more active the seeds in the seed box, the more likely they are to enter the large seed spoon. Therefore, the average velocity and average angular velocity of the seeds can detect the population activity. As multiple seeds picked up can significantly reduce overtime, the possibility of missing seeds increases. Therefore, the number of seeds picked by the large seed spoons should be known to detect the potato number. As the single seed rate is an important indicator of the metering seed device, the number of cleared seed particles by the small scoop needs to be detected and is given by the number of crossings.

Particle-contact model

We used the Longshu No.10 potato variety (Gansu, China) in this research. The water content in this variety, measured using the drying method (drying oven, DHG-9013A, Shanghai Yiheng Instruments Ltd., China), was 50.4%. Because the potato skin has good water resistance, the interparticle adhesion between particles was ignored, and Hertz-Mindlin (no slip) model (HMCM) was selected to simulate the motion behaviour between particles. This model simplifies the tangential and normal contact forces into parallel connections of springs and dampers, respectively (Fig. 2).

The normal and tangential forces, F_{n} and F_{t}, respectively, are defined as follows,

$$F_n = F_n^s + F_n^d \tag{1}$$

$$F_t = F_t^s + F_t^d \tag{2}$$

where F^s and F^d represent the contact and damping forces.

The contact models ensure that the magnitude of the total contact force in the tangential direction F^t does not exceed the maximum force caused by friction, as stated by Coulomb's law of friction,

$$F_t = \begin{cases} F_t \ \ if\, F_t < \mu \cdot F_n \\ \mu \cdot F_n^s \, if\, F_t \geqslant \mu \cdot F_n \end{cases} \tag{3}$$

where μ is the friction coefficient.

The gravitational force is added to F_n and F_t to calculate the resultant force (F_{res}) as follows:

$$F_{res} = F_n + F_t + mg \tag{4}$$

where m is the mass of the particle, and g is the gravitational acceleration. The tangential component of the contact force results in a moment (M), the magnitude of which is calculated as,

$$M = r_{con} \cdot F_t \tag{5}$$

$$\frac{1}{r_{eq}} = \frac{1}{r_a} + \frac{1}{r_b}$$

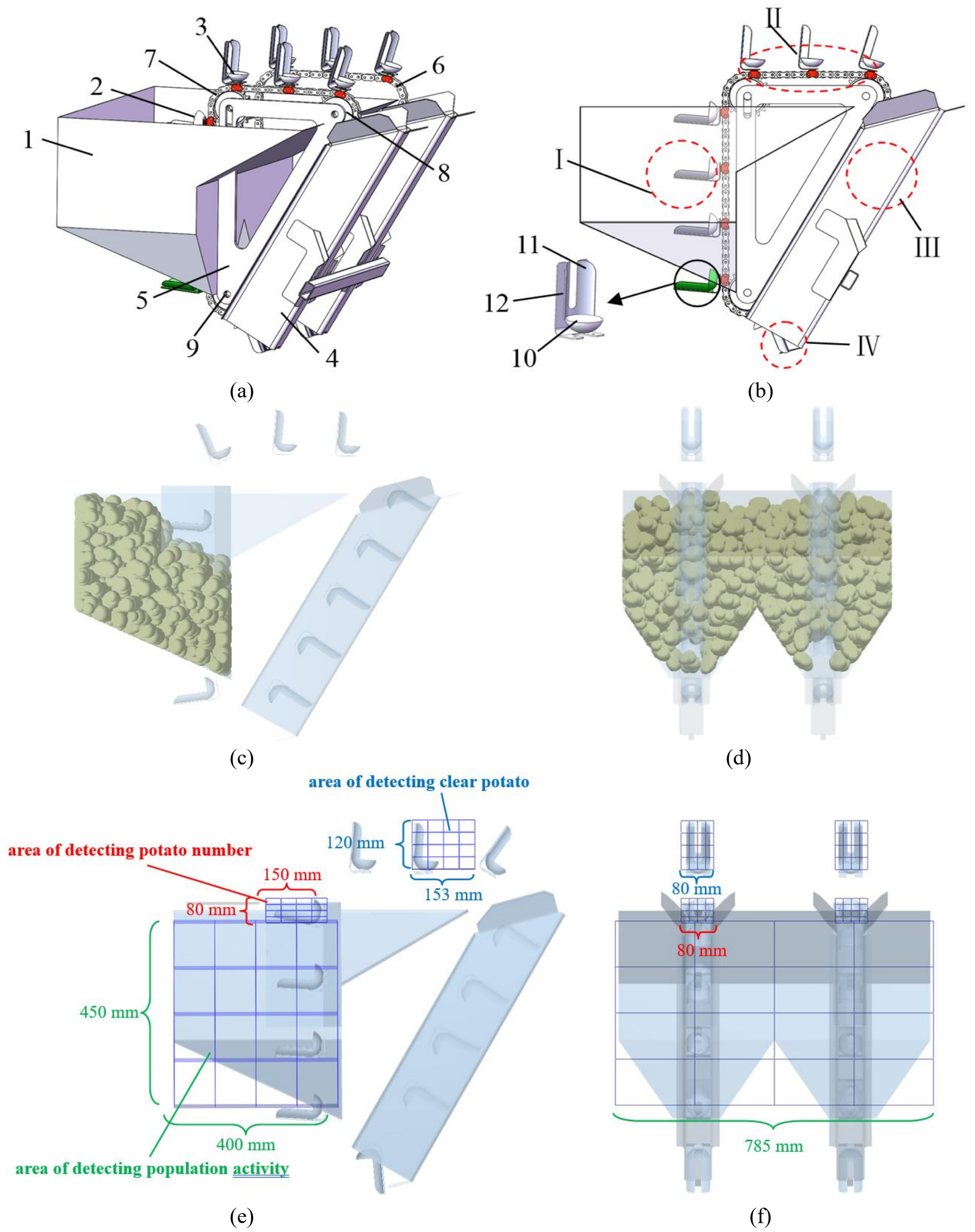

Figure 1. Potato cross-bridge metering device: (a) main view, (b) functional area division (I, seed-collecting stage; II, bridging stage to clear excess potatoes; III, seed carrying stage; IV, zero-speed throwing seed stage), (c) model of potato metering device, (d) division of detection area, (e) Location and dimensions of the three detection zones in left view, (f) Location and dimensions of the three detection zones in front view. 1, seed box; 2, seed spoon assembly; 3, spoon chain rack; 4, seed carrying box; 5, seed separator; 6, drive chain; 7, sprocket i; 8, sprocket ii; 9, sprocket iii; 10, small spoon; 11, large spoon; 12, scoop rack).

where r_{con} is the perpendicular distance of the contact point from the centre of mass; r_a and r_b are the radius of the individual particles *a* and *b*, respectively, and r_{eq} is the equivalent radius.

In a granular system, the rolling resistance also dissipates energy during the relative rotation and provides "packing support" that provides stability to the system. Therefore, an additional moment is also applied to the contacting surfaces as,

$$M_r = -\mu_r \cdot F_n^s \cdot r_{con} \cdot \lambda_{\dot{\theta}} \tag{6}$$

where M_r is the moment due to rolling friction, μ_r is the RF, and $\lambda_{\dot{\theta}}$ is the unit vector of angular velocity ($\dot{\theta}$) at the contact point. The resultant moment (M_{res}) is then obtained as the vector sum as follows:

$$M_{res} = M + M_r \tag{7}$$

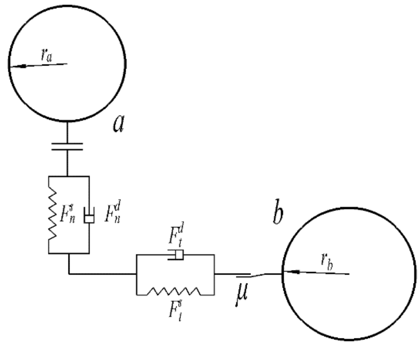

Figure 2. Particle contact model: r_a, r_b are the radius of the individual particles a and b, respectively F_n^s, F_t^s represent the normal and tangential contact forces, respectively; F_n^d, F_t^d represent the normal and tangential damping forces, respectively.

For updating the new position of the particle, the acceleration of the particle is calculated using Newton's second law of motion as follows:

$$\ddot{U} = \frac{F_{res}}{m} \tag{8}$$

$$\ddot{\theta} = \frac{M_{res}}{I} \tag{9}$$

where $\ddot{U}$, $\ddot{\theta}$, m, and I are the translational acceleration, rotational acceleration, particle mass, and moment of inertia of the particle, respectively. After calculating the velocity, the new positioning of the particle is computed by integrating the velocity over the time interval.

In HMCM, normal and tangential contact and damping forces between two particles are defined as,

$$F_n^s = -K_n \cdot U_{abn}^{3/2} \tag{10}$$

where U_{abn} is the normal component of the relative displacement, and K_n is the normal stiffness defined as,

$$K_n = 2 \cdot E_{eq} \cdot \sqrt{r_{eq} \cdot U_{abn}} \tag{11}$$

$$\frac{1}{E_{eq}} = \frac{\left(1-v_a^2\right)}{E_a} + \frac{\left(1-v_b^2\right)}{E_b}$$

where E and v are Young's modulus and Poisson's ratio, respectively, of the individual particles a and b.

The tangential contact force and stiffness K_t were defined by Mindlin (1949) as,

$$F_t^s = -K_t \cdot U_{abt} \tag{12}$$

$$K_t = 8 \cdot G_{eq} \cdot \sqrt{r_{eq} U_{abn}} \tag{13}$$

$$\frac{1}{G_{eq}} = \frac{2-v_a}{G_a} + \frac{2-v_b}{G_b}$$

where U_{abt} is the tangential component of the relative displacement; G_a, and G_b are the shear modulus for the individual particles a and b, respectively; and G_{eq} is the equivalent shear modulus.

The normal and tangential damping forces were determined as,

$$F_n^d = -2 \cdot \sqrt{\frac{5}{6}} \cdot \psi \cdot \sqrt{K_n \cdot m_{eq}} \cdot \dot{U}_{abn} \tag{14}$$

$$F_t^d = -2 \cdot \sqrt{\frac{5}{6}} \cdot \psi \cdot \sqrt{K_t \cdot m_{eq}} \cdot \dot{U}_{abt} \tag{15}$$

$$\frac{1}{m_{eq}} = \frac{1}{m_a} + \frac{1}{m_b}$$

$$\psi = \frac{\ln e}{\sqrt{\ln^2 e + \pi^2}}$$

where e is the coefficient of restitution of the particles; ma and m_b are the mass of the individual particles a and b, respectively; and m_{eq} is the equivalent mass.

Potato model

The classification of potato shapes is necessary as the flow will vary depending on the shapes and seeds. Therefore, 500 potatoes were randomly selected and the dimensions measured using a digital vernier calliper. The potato shape index was calculated using Eq. (16) to differentiate the three types of shape index (spherical, ellipsoidal, irregular) (Sang *et al.*, 2008; Jia *et al.*, 2011; Gu *et al.*, 2013), which were in a ratio of 238:233:29. The average length, width, and height of potato seeds were 89.5 mm, 74 mm, and 63 mm, respectively.

$$f = \frac{L^2}{WT} \times 100 \tag{16}$$

where f is the shape index, and L, W, and T are the maximum length, width, and height of potato seeds in mm, respectively.

The model of elliptical rice particles constructed by filling overlapping spheres has been studied and proven to be useful (Markauskas *et al.*, 2010). Accordingly, we modelled the three shape types of the potato seed using Solidworks 2018 SP5.0 (Dassault Systeme, USA) to the measured statistical size. The specific modelling process is as follows: the potato is cut along the maximum contour in the x-y section. The cut surface is fitted with white paper, and the contour is drawn with a pencil. Finally, the potato is divided into multi-layers along the y-z section. Image acquisition is achieved by adding a ruler perpendicular to the paper. The image is then imported into AutoCAD, and the potato is outlined using the spline curve command. The top-down sequences of potato slices are inserted into the corresponding datum level one by one. The outline of the whole potato is then imported into Solidworks, and the potato modelled using the lofting command (Shi *et al.*, 2013). The three potato model shapes imported into EDEM 2017 for particle filling are shown in Fig. 3.

Simulation parameters

A simulation was performed to obtain essential contact parameters such as RF, SF, and the coefficient of restitution. Because the Hertz-Mindlin model (Wang *et al.*, 2015) was used to simulate particle flow characteristics, the basic physical and mechanical contact parameters of the particles were determined first. The basic physical parameters, including shape classification, density, shear modulus, Poisson's ratio, and volume density, were determined using physical experiments as follows: average density was 1 048 kg m^{-3}, volume density was 631.88 kg m^{-3}. Poisson's ratio was 0.576, and modulus of elasticity was 4.42 MPa (Shi *et al.*, 2018). The contact parameters of potatoes, such as SF, RF, and the coefficient of restitution, were measured using the device developed herein.

Coefficient of static friction

SF significantly influences the interaction between the potato and contact body. The static friction between potato and two other materials (steel and plastic) is measured using the developed device (Fig. 4) as follows. The potato is placed on the movable plate. One end is connected to the thin wire through screws, and the other end passes through the pulley to the small bucket. When the power supply is switched ON, the lifting device moves to adjust the height of the potato. The power supply is disconnected when the thin wire is aligned horizontally to the potato. The position of the potato on the movable plate was moved so that the distance between the potato and photoelectric sensor connecting line was about 1 mm. One end of the solenoid valve hose (normally open) is placed directly above the bucket, and the electronic scale is placed directly below the bucket. When the manual switch is turned ON, the water in the tank flows through the manual switch and solenoid valve successively into the small bucket. When the gravity of the water in the bucket is equal to the force of static friction between the potato and movable plate (the flat plate was made with various materials, such as the same variety of potato, 45 steel, and plastic), the potato slides

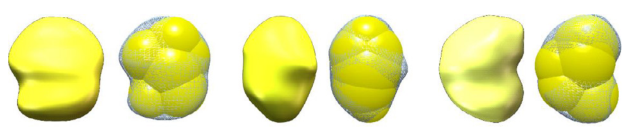

Figure 3. Three modes and discrete element model of particles: (a) round, (b) oval, (c) irregular.

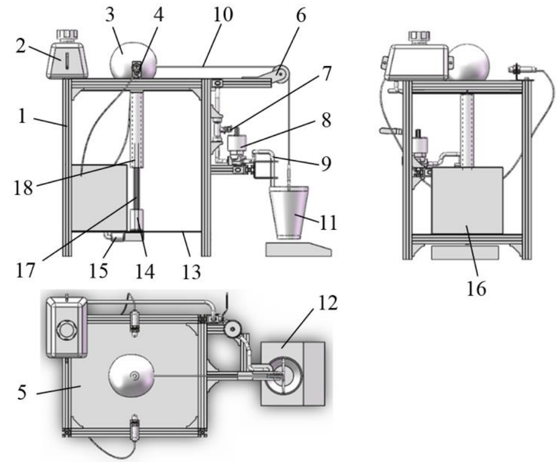

Figure 4. Measurement device of the coefficient of static friction: 1, frame; 2, water tank; 3, potato; 4, photoelectric sensor; 5, movable plate; 6, pulley; 7, switch; 8, solenoid valve; 9, hose; 10, thin wire; 11, bucket; 12, electronic scale; 13, bottom plate; 14, fixed ring; 15, motor; 16, control box; 17, screw; 18, nut sleeve.

forward to block the photoelectric sensor. The solenoid valve then closes the water flow channel of the hose and manual switch. The gravity of the potato and the bucket filled with water was measured by electronic scale. SF between potato and contact was obtained using Eq. (17) and given in Table 1.

The friction force is equal to the multiplication of the potato gravity and the friction coefficient:

$$\mu = m_1 g \,/\, mg \tag{17}$$

where μ is the coefficient of static friction between the potato and contact material, m is the mass of the potato in g, and m_1 is the mass of the water and bucket in g.

Coefficient of restitution

The coefficient of restitution (e) can affect the normal damping of the contact particles (Bharadwaj *et al.*, 2010) as they are highly influenced by the moisture content (Guo *et al.*, 2012); *e* is defined as the absolute ratio of the velocity after the collision to that before collision. We developed a new platform to measure the potato *e* (Fig. 5). The potato is placed in the pneumatic opening and closing mechanism. When the pneumatic switch is ON, the potato is dropped onto the drop tray, and the impact force is measured by the impact force sensor. Simultaneously, the impact contact area between the potato and contact plate is recorded on the carbon paper covering the drop tray. In addition, a high-speed camera collects the rebound height of the potato and the trajectory as it bounces away from the drop tray.

However, when the angle between the support plate and horizontal plane was 0º and the drop height of potato was 600 mm, we used Eq. (18) to calculate *e* (Table 2).

Table 1. Coefficients of static friction of potatoes

With soil	Particles		Particle and plastic		Particle and steel	
	Average value	SD	Average value	SD	Average value	SD
Yes	0.442	0.036	0.496	0.021	0.420	0.029
No	0.483	0.027	0.526	0.027	0.455	0.041

$$e = -\frac{\mu_n}{v_n} = \sqrt{\frac{h}{H}} \tag{18}$$

where μ_n and v_n are the normal velocities of potato after and before collision in m s^{-1}; H and h are the drop and rebound heights of potato in m, respectively.

RF between particles and contact material

The rolling friction angle is one of the most important design parameters of the potato seeder and is measured using the inclined plane method. The measurement platform is shown in Fig. 6. The process of measuring RF between a potato and the plate (made of plastic or steel) is as follows. When the potato is placed on the plate, the angle between the plate and horizontal plane gradually increases. When the potato begins to roll along the plate, the step motor is shut, and angle θ is recorded. The measurement was done thrice for each group of plates, and the results are given in Table 3.

Prediction of RF between particles

The simulation prediction method is used to calibrate RF (Wang *et al.*, 2015; Wang YX *et al.*, 2016) despite the differences between the actual and simulated potatoes in shape and centroid. This is because it is difficult to directly measure the RF between the particles experimentally. The RF of particles was changed to accumulate the repose angles under the same conditions (a steel drum with diameter 220 mm × height 300 mm), and three sets of experiments were carried out. We measured four repose angles in two directions for a stable repose angle. A relationship between the repose angle and RF was established (Fig. 7).

The repose angle was found to increase gradually with increasing RF. Fig. 8 shows the actual and simulated repose angles (24.72° and 24.39°, respectively) with a relative error of 1.33%. The bottom edge length and height of the simulated repose angle were 436 mm and 99 mm, respectively.

The predicted RF of particles is 0.022 (Eq. 19) when the repose angle is 24.76°. The parameters needed for the potato metering simulation are shown in Table 4.

$$y = 253.43\, x + 19.01 \tag{19}$$

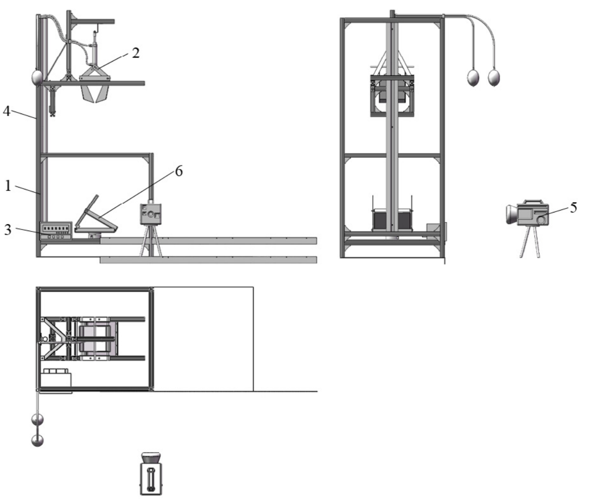

Figure 5. Platform to measure the potato coefficient of restitution: 1, frame; 2, pneumatic opening and closing mechanism; 3, drop experiment sensor; 4, height adjustment chute; 5, high-speed camera; 6, drop tray.

Factors and index of metering seed simulation experiment

The coefficient of friction between a particle and device (static/rolling) has a significantly lower effect on the simulation results than that between two particles (Bharadwaj *et al.,* 2010). A single-factor simulation experiment was performed to investigate how RF and SF affect the potato motion behaviour during metering seed. Table 4 shown that the maximum initial single-dimensional ranges were 0.01-0.12 and 0.1-1 for RF and SF, respectively. Therefore, the simulation factors of RF were set to 0.01, 0.06, and 0.12, and those of SF were set to 0.1, 0.5, and 1. The experimental indexes are selected from the requirements of potato planter experiment method (GB/T 6242-2006), and the qualified rate of single seed, D, and the rate of missing seed, M1, were calculated using Eqs. (20) and (21), respectively. Simulations and experiments were conducted in five groups of 32 sampling points each.

$$D = \frac{n_1}{n} \times 100\% \tag{20}$$

$$M_1 = \frac{n_2}{n} \times 100\% \tag{21}$$

Table 2. Potato coefficients of restitution

Contact material	Quality (g)	Bounce height (mm)	Contact area (mm²)	Impact force (N)	Coefficient of restitution	SD
Plastic plate	153.38	145.60	508.06	5.81	0.49	0.02
Steel plate	142.56	117.4	421.94	5.12	0.44	0.07
Soil	149.52	15.2	3335.37	3.34	0.15	0.04
Potato particle	149.48	86.4	461.34	5.09	0.37	0.09

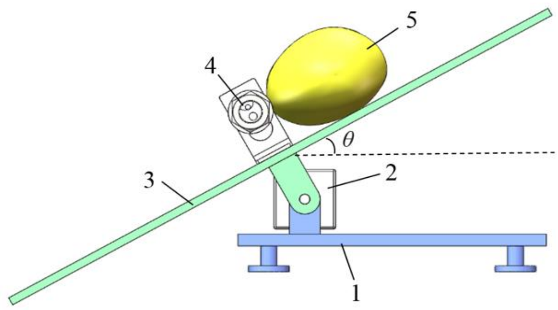

Figure 6. Measurement device of the angle of rolling friction (θ, in °) between potato particle and other materials: 1, support base; 2, step motor; 3, plate; 4, photoelectric sensor; 5, potato.

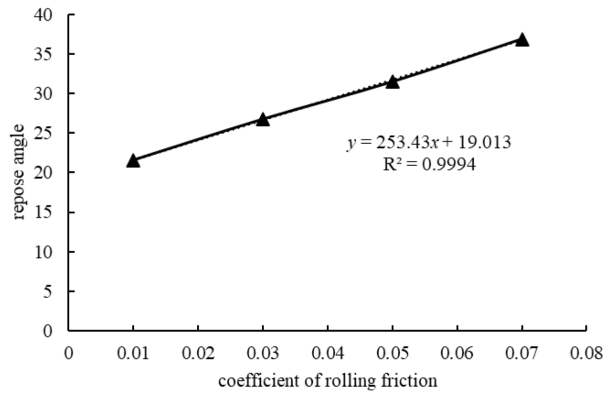

Figure 7. Relationship between RF and repose angle

where n_1 and n are the number of metering single seed and all particles, respectively, and n_2 is the number of missing seed.

Results

The above analysis shows that SF and RF follow the order: particle and plastic > particle and steel > particles, and are lesser in potatoes with soil than that without soil. Therefore, RF and SF vary according to the conditions of the potato surface soil. It is necessary to study the influence of both factors on seed metering performance to improve the soil content of the potato seed surface through artificial modification.

Process of potato metering

The potato metering process using the cross-bridge metering device is shown in Fig. 9. Fig. 9a shows that the particles are generated in the seed box within 1 s. After 1 s, the rotating drive chain pushes the particles in the seed box upward using the large spoon while overcoming the resistance of other seeds When the seed spoon assembly leaves the potato population, a limited number of particles in them are separated, and they continue to move with the drive chain (Fig. 9b). Because the large spoon has an effective area larger than the small spoon and an inconsistent angular velocity in its length direction, some particles slide from the large spoon to the small spoon and are dropped back into the seed box as the seed spoon assembly rotates through sprocket I (Fig. 9b). As the simulation proceeds, the angle between the large spoon and the horizontal plate is such that the particles roll down the seed spoon assembly. When the seed spoon assembly passes through sprocket II, a potato in the small spoon fall on the back of the former large spoon in the seed carrying box and moves down towards the outlet (Figs. 9c-e). As the simulation proceeds, the number of potato particle in the seed box decreases (Fig. 9f).

Table 3. Coefficient of rolling friction between potato particle and plastic, steel

With soil	Particle and plastic		Particle and steel	
	Average value	SD	Average value	SD
Yes	0.327	0.10	0.256	0.05
No	0.413	0.06	0.312	0.04

Model validation

To verify the reliability of the parameters of the potato metering process design, an experimental bench was developed (Fig. 10). The experimental conditions were the same than in the simulations. The hemispherical small spoon had a maximum diameter of 59 mm,

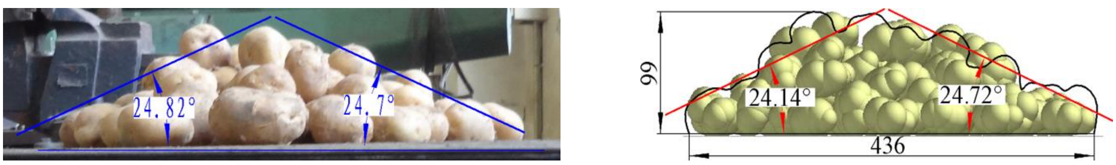

Figure 8. Repose angle of particles: (a) actual and (b) simulated.

Table 4. Physical and contact parameters

Parameters	Value	Source
Poisson ratio of seed potatoes	0.57	Measured
Shear modulus of seed potatoes (MPa)	1.336	Measured and calculated
Seed potatoes density (kg m^{-3})	1 048	Measured
Poisson ratio of steel	0.30	Shi *et al.* (2018)
Shear modulus of steel (Pa)	7×10^{10}	Shi *et al.* (2018)
Steel density (kg m^{-3})	7800	Shi *et al.* (2018)
Poisson ratio of plastic	0.35	Shi *et al.* (2018)
Shear modulus of plastic (Pa)	1.3×10^{9}	Shi *et al.* (2018)
Plastic density (kg m^{-3})	1.20	Shi *et al.* (2018)
Coefficient of restitution between seed potatoes	0.79	Feng *et al.* (2017)
Coefficient of restitution between seed potatoes and steel	0.71	Feng *et al.* (2017)
Coefficient of restitution between seed potatoes and plastic	0.66	Feng *et al.* (2017)
SF between seed potatoes and plastic	0.517	Measured
SF between seed potatoes and steel	0.445	Measured
RF between seed potatoes and plastic	0.301	Measured
RF between seed potatoes and steel	0.269	Measured
SF of potatoes	0.1-1	Measured
RF of potatoes	0.01-0.12	Model prediction

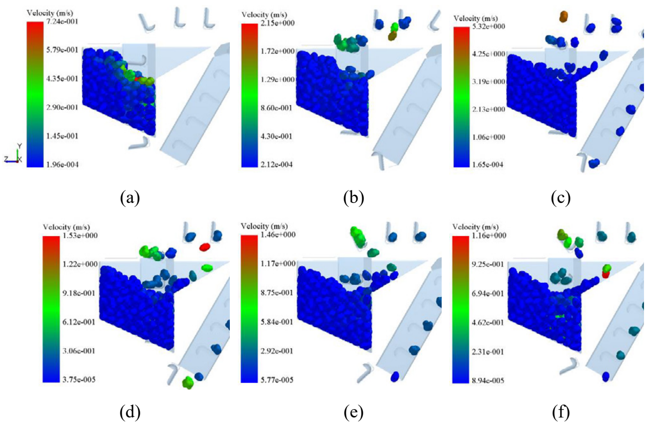

Figure 9. Potato metering process of bridge seeding device: (a) 1 s, (b) 3 s, (c) 6 s, (d) 9 s, (e) 12 s, and (f) 15 s

Figure 10. Experimental table of potato cross-bridge metering device

Table 5. Experiment and simulation results

Index	Simulation value	Experiment value
Rate of metering single seed, %	98.17	97.57
Rate of missing seed, %	1.83	2.43

depth of 22 mm, and a circular hole of 15 mm at its bottom. The semicylindrical big spoon was 59 mm in diameter, 90 mm in height, and 22 mm in thickness. The spacing between the spoons was 152.4 mm. The drive chain was set at 0.6 m s^{-1}, and the experiment was repeated three times.

Table 5 shows the experiment and simulation results of seed metering, and the results were averaged. The relative error in the rate of metering single seed in simulation and experiment was 0.61%. Compared with the simulation results, the experiment rate of missing seed increased by 0.60% under the same conditions due to the increasing variations in potato size and other factors and shakes in the chain transmission process.

The results verify that the selected potato seed simulation parameters can generate reliable results for analysis. In the following sections, the effect of RF and SF on seed metering performance of the proposed cross-bridge metering device are analysed in-depth.

Influence of RF on the metering performance

Activity of potato seed particles in the seed box

The activity level of potatoes in the seed box will determine the probability of filling the large spoon with the seed particles. The degree of seed activity is mainly reflected by their instantaneous velocity and angular speed and is derived from two sources. First, as the seed scoop assembly travels through Sprocket I from below, it

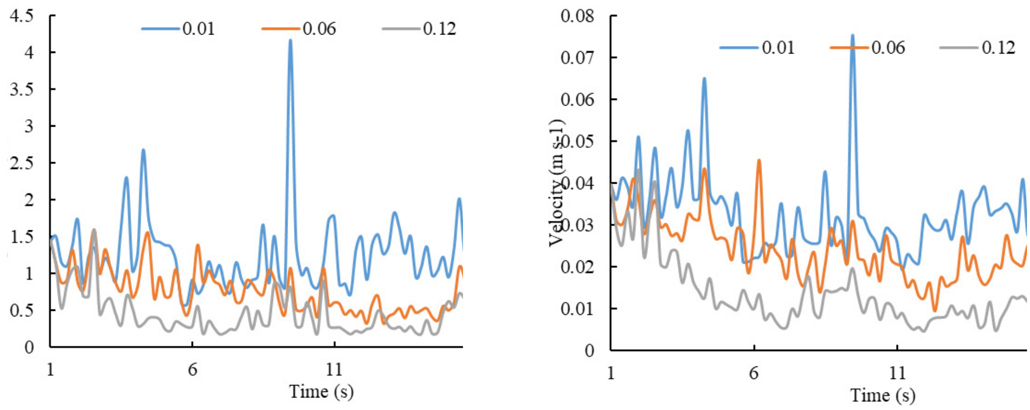

(a) (b)

Figure 11. Average velocity changes of potatoes in the seed box for different RF (0.01, 0.06, 0.12) and a constant SF of 0.045: (a) angular velocity and b) velocity.

Table 6. Analysis of variance (ANOVA)

Type	Impact indicators	Source of difference	SS	df	MS	F	*p*-value	F crit
RF	Angular velocity	Between groups	35.28917	2	17.64458	99.02326	1.32×10^{-33}	3.026466
		In group	52.38676	294	0.178186			
		Total	87.67592	296				
	Velocity	Between groups	0.020186	2	0.010093	146.7949	6.21×10^{-45}	3.026466
		In group	0.020214	294	6.88E-05			
		Total	0.0404	296				
SF	Angular velocity	Between groups	20.10640704	2	10.05320352	29.34498421	2.40033×10^{-12}	3.026465904
		In group	100.720512	294	0.342586776			
		Total	120.8269191	296				
	Velocity	Between groups	0.026968602	2	0.013484301	114.1199885	2.09002×10^{-37}	3.026465904
		In group	0.03473874	294	0.000118159			
		Total	0.061707342	296				

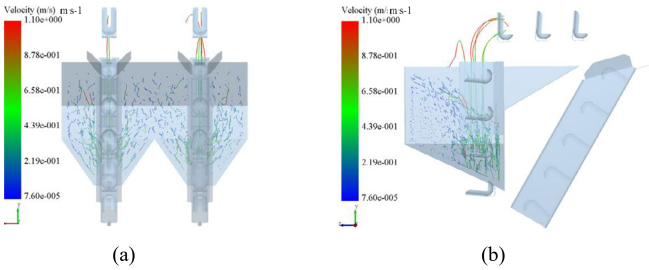

Figure 12. Stream display of particles during taking seed process: (a) main view, (b) side view.

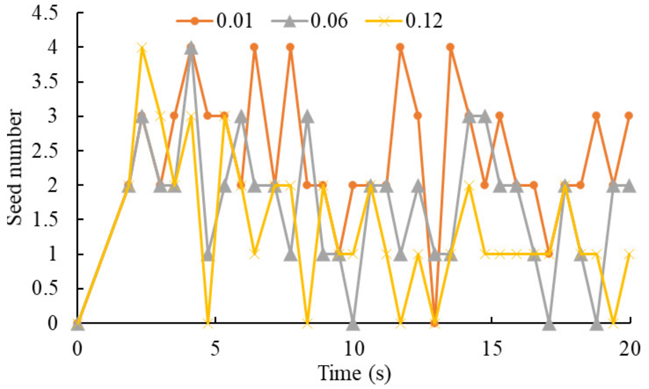

Figure 13. Seed number taken by the large spoon under different coefficient of rolling friction with time

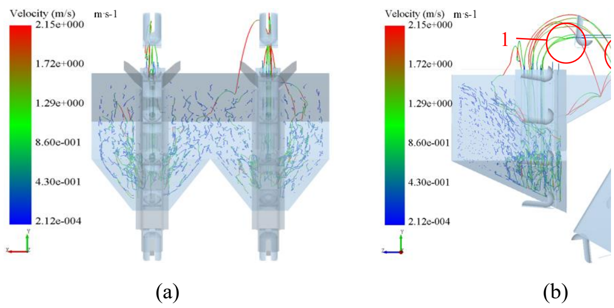

Figure 14. Stream display of seeds during clearing seed process: (a) main view and (b) side view. The red circle 1 indicates the method of clearing based on the angular velocity of seeds outside the large spoon. The red circle 2 indicates the trajectory of some seed fall into the seed box as they slide past through the bridging stage to clear excess potatoes.

disturbs the seed population around them. Second, when the large seed scoop picks the seed, the empty space is immediately filled by the neighbouring seed population from top to bottom under gravity. Because the seed population fills the seed box with the same height at the start of the simulation and seed scoop assembly moves upward at a certain speed, the external factors of metering are certain. Therefore, to quantify the effects of RF on the seed population motion in the seed box, the average resultant angular velocity and resultant velocity changes in the seed-collecting area were extracted (Fig. 11). As seen in Fig. 11, when SF is kept constant at 0.045, the average resultant velocity and angular velocity decrease with increasing RF (0.01, 0.06, 0.12). To analyse the significance of varying the seed RF on the level of population activity, ANOVA was conducted. Table 6 shows that RF had a highly significant effect on the average resultant velocity and angular velocity of the seed particles. To understand the effect of changing RF on the metering performance, further experiments were performed on the picking seed rate of the large seed scoop and clearing seed quality of the small seed scoop.

Seed number picked by the large seed spoon

The chance of seed particles picked by the large spoon affects the seeding performance of the qualified rate of single seed and rate of missing seed. The trajectory line of the seeds during the large seed scoop is shown in Fig. 12. To facilitate the study, the number of seeds taken and cleared was obtained from the left side of the seeder. The seed population in the seed box converges from top to bottom at the seed spoon assembly (Fig. 12a). The large seed spoon picks one or more seeds (Fig. 12b), and the remaining seed population at the bottom of the seed box slides from left to right. This further illustrates that the main movement of the seed population in the seed box is downward, which is opposite to the movement of seed spoon assembly and more conducive to seed filling. To investigate the picking seed frequency of large seed scoop and the influence of RF, the number of seed particles passing through the area of detecting potato was plotted under different RF (0.01, 0.06, 0.12) at a constant SF of 0.045 (Fig. 13).

The large seed spoon was missed one, three, and five times in 32 data points with increasing RF values of 0.01, 0.06, and 0.12, respectively. Therefore, increasing RF between potatoes increases the risk of potato missing. In addition, the average number of seeds picked by the large seed scoop decreased and was 2.47, 1.75, and 1.41 at RF values of 0.01, 0.06, and 0.12, respectively. The number of potato seeds picked should not be too much or too less; too many seeds will increase the load of the seed clearing process and very less number of seeds will increase the possibility of missing seeds. When RF was 0.06, the potato number was relatively consistent, and particles did not show apparent discharge and discontinuity. At RF of 0.01, the potato number fluctuated significantly. Because increasing RF restricts the motion of particles, the particle velocity and angular velocity decreased and spoon filling ability reduced.

The seed clearing rate is also an important performance indicator of the metering seed device, and the effect of different RF on seed clearing rate was investigated. The number of particles taken by the large spoon in the previous step will affect the clearing process. There are two main methods to clear excess seeds (Fig. 14). In the first method, because the angular velocity of seeds outside the large spoon is relatively large, some seeds will be thrown out during rotation. In the second method, the excess seeds will slide past the small spoon and fall back into the seed box. The number of seeds passing through the area of detecting clear potato was plotted. Fig. 15 shows that, the number of missing seeds were 1, 3, and 14 at RF values of 0.01, 0.06, and 0.12, respectively. The seed number in the small seed scoop after clearing seeds was 1 in the three cases. Moreover, the missing seed number picked by the large seed spoon and the number of missing seed after the clearing process were 1 at 0.01 RF and 3 at 0.06 RF. However, for 0.12 RF, the missing seed number picked was 5, and the seed number after the clearing process was 14, *i.e.*, the rate of missing seed after the clearing process reached 62.28% of the overall rate of missing seed. Thus, changes in RF had little effect on clearing seeds at low RF values.

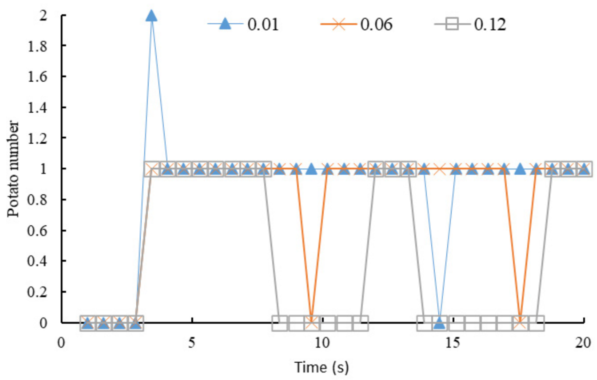

Figure 15. Seed number under different coefficient of rolling friction during clearing seed process

Influence of SF on the metering performance

Activity of potato seed particles in the seed box

For analysing the effects of SF on seeds motion in the seed box, the seed average angular velocity and resultant velocity changes in the seed-collecting area were extracted, keeping the RF constant. Fig. 16 shows that the average resultant angular velocity and velocity decrease with increasing SF. To analyse the significance of the effect of changing SF on population activity, an ANOVA was conducted. Table 6 shows that SF had a significant effect on the potato angular velocity and velocity in the seed box. Further observations are needed to understand the effect of SF on the picking seed rate of the large seed scoop and the clearing seed quality of the small seed scoop.

Seed number picked by the large seed spoon

To investigate the picking seed frequency of large seed scoop and multiple seeds number influenced by SF, the number of seed particles passing through the area of detecting potato was plotted under different SF (0.1, 0.5, 1), keeping the RF constant at 0.22.Fig. 17 shows that, at 0.022 RF, the large seed spoon missed zero times in the 32 data points in all SF cases. The average number of seeds taken by the large seed scoop were 4.33, 2.16, and 2.12 for SF values of 0.1, 0.5, and 1.0, respectively. Thus, with increasing SF (0.1, 0.5, 1), the number of potatoes taken by the large spoon first decreased and gradually levelled off. At RF of 0.1, the potato number fluctuated significantly. Because the increasing static friction force restricts the motion of particles, the particle velocity and angular velocity decreased, and reduced the ability to fill the spoon.

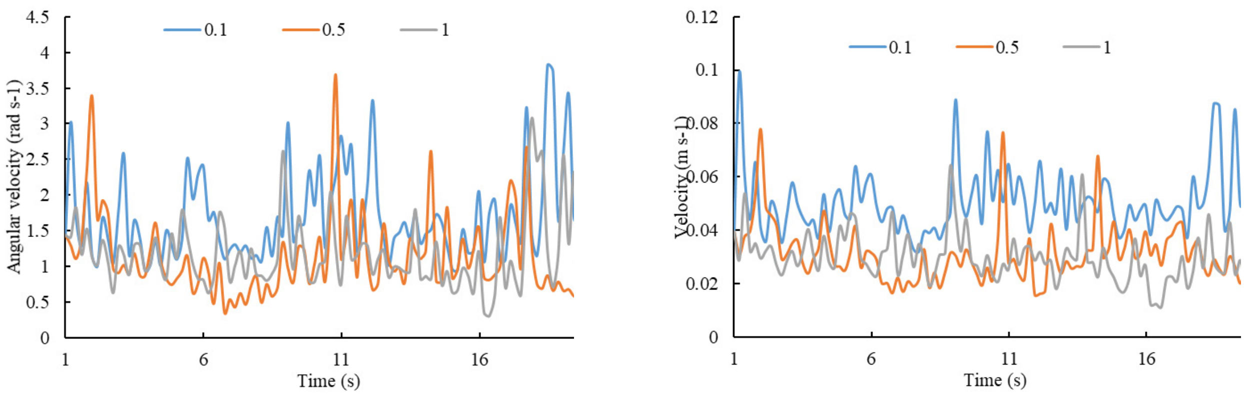

(a) (b)

Figure 16. Velocity changes of potatoes in the seed box for SF values of 0.1, 0.5, and 1: (a) angular velocity and time (b) velocity and time. RF was kept constant at 0.22 under all conditions.

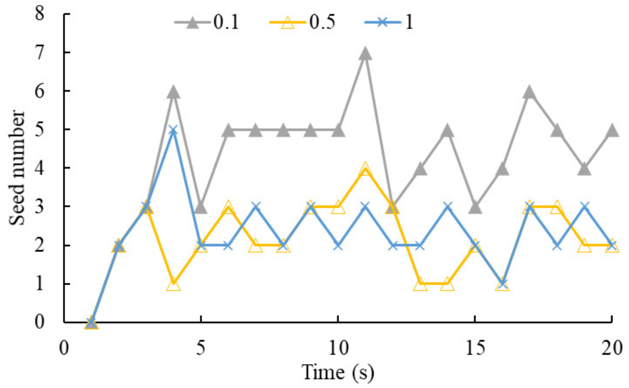

Figure 17. Seed number picked by the large spoon under different coefficient of static friction with time. RF was kept constant at 0.22.

Success rate of clearing particles

The number of seeds passing through the area of detecting clear potato at 0.22 RF was plotted. Fig. 18 shows that. The number of missing seeds was 0, 3, 16 when SF was 0.1, 0.5, and 1.0, respectively. The seed number in the small seed scoop after clearing seed also was 1 in the three cases. Moreover, when SF was 0.1, the missing seed number taken by the large seed spoon was 0, and the seed number of missing seed after the clearing process was 0. When the seed number was 0.5, the missing seed number taken was 0, and the seed number after clearing process was 3. When SF was 1, the missing seed number taken was 0, and the seed number after the clearing process was 16. The rate of missing seed after the clearing process reached 100% of the overall rate of missing seed. Thus, the change of SF had a strong influence on clearing seeds.

Discussion

In this work, the effect of the contact parameters of seed particles SF and RF on the performance of the proposed cross-bridge metering device was investigated in detail. The experiments show that the surface of seed particles with and without soil can change the magnitude of SF and RF. To investigate the effect on the metering performance using the potato cross-bridge metering device, it is necessary to study the effect of RF and SF on the velocity and angular velocity of seed particles in the seed box, the potato number being taken by the large spoon in taking seed and in clearing seed process. The following conclusions can be drawn from the present work:

SF and RF were measured by build-in devices, which is an improvement over the current mature measurement methods, such as the traditional slope method with large error and complicated operation process. The results show SF and RF of the potato seed with soil are smaller than those without soil and decrease in the following order: potato seed and plastic > potato particle and steel > seed particles. A single-factor simulation experiment was performed to investigate the effect of SF and RF on the motion of seed particles. On the one hand, the results show that with increasing RF (0.01, 0.06, 0.12), the resultant angular velocity and velocity of the seed particles in the seed box decrease significantly. In general, the results were like in Wang et al, 2018, the increase in the coefficient of rolling friction constrains the increase in rotational kinetic energy of corn seeds. In addition, the number of seed particles taken by the large spoon during the seed-collecting stage I decreases due to the rolling friction force restricting the rotating ability of seed particles to fill the large spoon. Besides, the increasing RF of seed particles has little impact on clearing seed particles during the bridging stage II. On the other hand, the coefficient of static friction can significantly affect the linear and rotational motion of rice particles (Zeng *et al.,* 2018). When SF increases, potato seed velocity in the seed box significantly decreases, while the resultant velocity indistinctly decreases. The number of seed particles taken by the large spoon during the seed-collecting stage I also decreases with increasing SF. The increasing SF can also restrict clearing excess particles, even causing reseeding. The potato surface with or without soil affects its contact mechanics parameters, further impacting the metering seed performance of the cross-bridge metering device, which can be improved by artificially increasing the soil content on the potato surface. The results shed light on the need for potato seed surface treatment for mechanised metering.

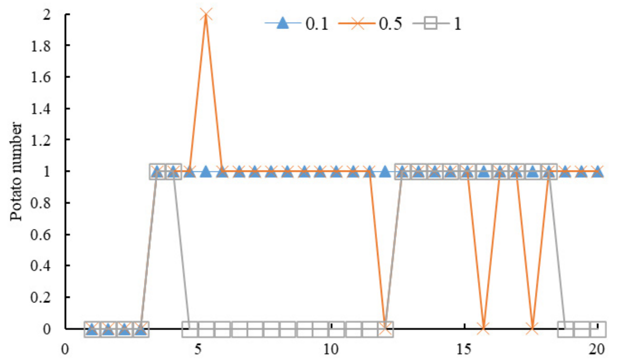

Figure 18. Seed number cleared under different coefficients of static friction with time.

References

Al-Gaadi KA, Marey SA, 2011. Effect of forward speed and tuber characteristics on tuber spacing uniformity for a cup-belt potato planter. Middle-East J Sci Res 8 (4): 753-758.

Barr JB, Ucgul M, Desbiolles J, Fielke JM, 2019. Development and field evaluation of a high-speed no-till seeding system. Soil Till Res 194(1): 104337. https://doi.org/10.1016/j.still.2019.104337

Bharadwaj R, Ketterhagen WR, Hancock BC, 2010. Discrete element simulation study of a freeman powder rheometer. Chem Eng Sci 65(21): 5747-5756. https://doi.org/10.1016/j.ces.2010.04.002

Buitenwerf H, Hoogmoed WB, Lerink P, Müller J, 2006. Assessment of the behaviour of potatoes in a cup-belt planter. Biosyst Eng 95(1): 35-41. https://doi.org/10.1016/j.biosystemseng.2006.06.007

Du HW, Shang SQ, Yang RB, Wang DW, 2011. Research and analysis on mechanized seed potatoes sowing techniques. J Agr Mechan Res 33(2): 214-217.

Feng B, Sun W, Shi LR, Sun BG, Zhang T, Wu JM, 2017. Determination of potato tuber collision recovery coefficient and analysis of influencing factors. T CSAE 33(13): 50-57.

Gao GH, Xie HF, 2019. Numerical analysis and simulation of potato soil separation mechanism based on EDEM. J Agr Mechan Res 41(01): 15-21.

Gu LX, Wang CG, Liu HC, Wang J, Fu Y, 2013. Simulation analysis on irregular potatoes modeling based on pro/E5.0. J Agr Mechan Res 34(12): 32-35.

Guo WB, Wang CG, Gao JJ, 2012. Study on correlation between the starch content of potato tuber and its viscoelastic characteristics. Adv Mater Res 591-593: 2545-2550. https://doi.org/10.4028/www.scientific.net/AMR.591-593.2545

Hamid A, Ahmad D, Rukunuddin IH, 2010. Performance of sweet potato transplanting machine on mineral and bris soils. Agr Mech Asia Afr Latin Am 41(1): 55-59.

Hou JL, Liu W, Zhang WZ, Lv JQ, Lv ZQ, Zhang ZL, 2018. Design of precision pneumatic cup seed-metering device for potato. T CSAE 34(24): 18-28.

Jia JX, Yang DQ, Zhang DX, 2011. Moving simulation analysis on potato tuber during harvester. J Agr Mechan Res 33(8): 38-41.

Lei XL, Hu HJ, Wu WC, Liu HN, Liu LY, Yang WH, *et al.*, 2021. Seed motion characteristics and seeding performance of a centralised seed metering system for rapeseed investigated by DEM simulation and bench testing. Biosyst Eng 203(22): 22-33. https://doi.org/10.1016/j.biosystemseng.2020.12.017

Li HC, Li YM, Tang Z, Xu LZ, Zhao Z, 2011. Numerical simulation and analysis of vibration screening based on EDEM. T CSAE 27(5): 117-121.

Li QZ, 2008. The economic analysis of potato production in China. Huazhong Agri Univ.

Liu WZ, He J, Li HW, Li XQ, Zheng K, Wei ZC, 2018. Calibration of simulation parameters for potato minituber based on EDEM. T CSAM 49(05): 125-135, 142.

Liu WZ, He J, Li HW, Li XQ, Lu CY, Wei ZC, Wang CL, 2019. Seeding performance optimization on vibration-arranging type seeding device for potato micro-seed. T CSAE 35(7): 1-11.

Lu XP, 2015. Strategy of potato as staple food: significance, bottlenecks and policy suggestions. J Huazhong Agric Univ 3: 1-7.

Lv JQ, Wang ZM, Sun XS, Li ZH, Guo ZP, 2015. Design and experimental study of feed screw potato planter propulsion. J Agr Mechan Res 6: 194-196, 200.

Lv JQ, Yi SJ, Tao GX, Mao X, 2018. Parameter optimization and experiment of splitter sliding-knife opener for potato planter. T CSAE 34(4): 44-54.

Mindlin RD, 1949. Compliance of elastic bodies in contact. J Appl Mech 16(3): 259-268. https://doi.org/10.1115/1.4009973

Markauskas D, Kaianauskas R, 2011. Investigation of rice grain flow by multi-sphere particle model with rolling resistance. Granul Matter 13(2): 143-148. https://doi.org/10.1007/s10035-010-0196-5

Markauskas D, Kacianauskas R, Dziugys A, Navakas R, 2010. Investigation of adequacy of multi-sphere approximation of elliptical particles for DEM simulations. Granul Matter 12(1): 107-123. https://doi.org/10.1007/s10035-009-0158-y

Moreno-Atanasio R, 2012. Energy dissipation in agglomerates during normal impact. Powder Technol 223: 12-18. https://doi.org/10.1016/j.powtec.2011.05.016

Niu K, Yuan YW, Luo M, Liu YC, Lv CX, Fang XF, 2016. Design and experiment of potato metering device with double-deck seed tank. T CSAE 32(20): 32-39.

Owen PJ, Cleary PW, 2012. Prediction of screw conveyor performance using the discrete element method (DEM). Powder Technol 193(3): 269-282. https://doi.org/10.1016/j.powtec.2009.03.012

Pasha M, Hare C, Ghadiri M, Gunadi A, Piccione PC, 2016. Effect of particle shape on flow in discrete element method simulation of a rotary batch seed coater. Powder Technol 298: 29-36. https://doi.org/10.1016/j.powtec.2015.10.055

Peng F, Li TF, Kang HB, Zhang GD, Kong DD, Wang HY, 2016. Optimization and experiment on feeder for small-scale pellet mill. T CSAM 47(2): 51-58.

Sang YY, Zhang DX, Zhang MM, 2008. Study on bruising damage experiment of potato and finite element analysis. J Cn Agric Univ 13(1): 81-84.

Shi LR, Zhao WY, Wu JM, Zhang FW, Sun W, Dai F, Wang LJ, 2013. Application of slice modelling technology in finite element analysis of agricultural products. J Agr Mechan 34(3): 95-98.

Shi LR, Sun W, Zhao WY, Yang XP, Feng B, 2018. Parameter determination and validation of discrete element model of seed potato mechanical seeding. T CSAE 34(6): 35-42.

Wang LJ, Zhou W, Ding Z, Li X, Zhang C, 2015. Experimental determination of parameter effects on the coefficient of restitution of differently shaped maize in three-dimensions. Powder Technol 284: 187-194. https://doi.org/10.1016/j.powtec.2015.06.042

Wang XY, Tang H, Wang JW, Lv JQ, Li ZH, 2016. Optimized design and experiment on double-row cross spoon-belt potato precision seed metering device. T CSAM 47(11): 82-90.

Wang YX, Liang ZJ, Zhang DX, Cui T, Shi S, Li KH, Yang L, 2016. Calibration method of contact characteristic parameters for corn seeds based on EDEM. T CSAE 32(22): 36-42.

Wang LJ, Li R, Wu BX, Wu ZC, Ding ZJ, 2018. Determination of the coefficient of rolling friction of an irregularly shaped maize particle group using physical experiment and simulations. Particuology 38: 185-195. https://doi.org/10.1016/j.partic.2017.06.003

Wu ZJ, Li, ML, Lei XL, Wu ZY, Jiang CK, 2020. Simulation and parameter optimisation of a centrifugal rice seeding spreader for a UAV. Biosyst Eng 192: 275-293. https://doi.org/10.1016/j.biosystemseng.2020.02.004

Yan DX, Yu JQ, Wang Y, Zhou L, Yu YJ, 2020. A general modelling method for soybean seeds based on the discrete element method. Biosyst Eng 372: 212-226. https://doi.org/10.1016/j.powtec.2020.05.054

Yang QS, 2014. Analysis on the problems existing in potato planter elevate particles device. Mach Ind Std Qual 9: 35-37.

Yang RB, Yang HG, Shang SQ, Ni ZW, Liu ZS, Guo D, 2018. Design and experiment of vertical circular separating and conveying device for potato combine harvester. T CSAE 34(3): 10-18.

Zeng Y, Jia FG, Meng XY, Han YL, Xiao YW, 2018. The effects of friction characteristic of particle on milling process in a horizontal rice mill. Adv Powder Technol 29(5): 1280-1291. https://doi.org/10.1016/j.apt.2018.02.021

Zhang H, Xu F, Wu Y, Hu HH, Dai XF, 2017. Progress of potato staple food research and industry development in China. J Integr Agric 12: 2924-2932. https://doi.org/10.1016/S2095-3119(17)61736-2